Taylor & Francis
Taylor & Francis Group

Journal of Hydraulic Research

ISSN: (Print) (Online) Journal homepage: https://www.tandfonline.com/loi/tjhr20

Modelling marine turbine arrays in tidal flows

Peter K. Stansby & Pablo Ouro

To cite this article: Peter K. Stansby & Pablo Ouro (2022): Modelling marine turbine arrays in tidal flows, Journal of Hydraulic Research, DOI: 10.1080/00221686.2021.2022032

To link to this article: https://doi.org/10.1080/00221686.2021.2022032

Published online: 18 Feb 2022.

Journal of Hydraulic Research, 2022
https://doi.org/10.1080/00221686.2021.2022032

Vision paper

Modelling marine turbine arrays in tidal flows

PETER K. STANSBY, Osborne Reynolds Professor of Fluid Mechanics, IAHR Member, *Department of Mechanical, Aerospace and Civil Engineering, University of Manchester, Manchester M13 9PL, UK*
Email: p.k.stansby@manchester.ac.uk (author for correspondence)

PABLO OURO, Dame Kathleen Ollerenshaw Fellow, *Department of Mechanical, Aerospace and Civil Engineering, University of Manchester, Manchester M13 9PL, UK*
Email: pablo.ouro@manchester.ac.uk

ABSTRACT
Tidal stream turbines operate in the harsh marine environment, subjected to turbulence, wave action and wakes from upstream devices when deployed in arrays. Turbines may be mounted on the sea bed or on floating platforms. Numerical models are invaluable to study individual and array performance and their interaction with environmental flows. To date, shallow water models and three-dimensional Reynolds averaged Navier–Stokes (RANS) simulations predominate the simulation of turbine arrays, while large-eddy simulation (LES) is becoming more widely used due to availability of high-performance computing resources. The accuracy of turbine performance and load prediction depends on the ability to represent turbulence in the tidal flow and unsteady wake effects. Inclusion of waves increases the modelling complexity and is particularly significant for floating platforms. In this Vision Paper, we provide a perspective on the numerical approaches currently used for modelling tidal flows and marine turbines, suggesting future challenges envisaged in this field.

Keywords: Large-eddy simulation; marine turbines; modelling; turbine arrays; tidal flows

1 Introduction

Wind and marine turbines generate renewable energy with similar flow characteristics when in isolation. However, grid scale power generation requires turbines to be deployed in farms and interaction with wind and tidal flows differs quite notably. An advantage for wind energy is that the atmospheric boundary layer normally extends a kilometre or more above ground or sea level without an upper bounding surface, while tidal flows are usually on continental shelves with depths less than 100 m bounded by the water surface. This determines turbine size and downstream wake recovery, and hence farm layout.

An advantage of marine power is its predictability as defined by tidal cycles. A disadvantage is the hostile marine environment itself which can be highly turbulent with many scales, both large-scale bathymetry and bed-induced, with intermittent, superimposed oscillatory wave action. Deployment generally requires a period of slack tide within a benign weather window. Sea water is inherently corrosive and, in addition, promotes marine growth on structures. Both fixed and floating platforms are being developed as for offshore wind with subsea foundations or moorings for floaters. Importantly there are many sites worldwide where strong tidal currents, greater than 3 m s^{-1}, make marine turbines an attractive renewable energy option, with capacity order 1 MW and little visual intrusion. There are various sites under consideration in the UK and Channel Islands, France, USA, Canada, Korea, China amongst others. The world capacity is thought to be about 120 GW or 5% that of wind or wave with a large proportion, around 11.5 GW, in the UK (Coles et al., 2021; Offshore Energy, 2015).

There has been considerable effort on laboratory scale measurements of turbine flows, computational modelling and some limited field measurements. The basic fluid mechanics of turbines, wakes, and associated blockage is well understood and has been comprehensively reviewed in Adcock et al. (2021). Tidal modelling is a quite mature field with various 3D ocean models assuming hydrostatic pressure and accounting for the buoyancy effects due to salinity and temperature (within the Boussinesq assumption). Depth-averaged models are also used to reduce computation costs for some assessments. Different levels of coupling with turbine arrays are possible and this is one focus of this paper.

Received 13 September 2021; accepted 11 December 2021/Currently open for discussion.

ISSN 0022-1686 print/ISSN 1814-2079 online
http://www.tandfonline.com

We first present different levels of models for turbines and tidal flows with associated physical assumptions. Then the models' efficacy is assessed, followed by consideration of combination of tidal modelling with wave modelling. The modelling of fixed and floating platforms is then described. The paper concludes with suggested future modelling developments.

2 Turbine and tidal models

The various levels for modelling tidal stream turbines in tidal models are shown in Table 1.

2.1 *Turbine models*

In its most basic form the actuator disc is represented as a pressure drop extracting energy from the flow as shown in Fig. 1 (left). In one dimension, considering stream tubes, this elegantly gives the axial induction factor defining the change in velocity at the disc relative to free stream velocity (Betz, 1920; Glauert, 1935). This then defines the power and thrust coefficients, C_P and C_T, giving an upper limit for $C_{P\max} = 16/27$ known as the Betz limit. With blockage factor B (defined by the turbine swept area divided by channel cross-sectional area) this may be increased as $C_{P1\max} = (16/27)/(1-B)^2$ (Garrett & Cummins, 2013). This linear-momentum actuator disc theory has shown how maximum energy yield would increase when deploying turbines in fences, rows or with other arrangements (Draper & Nishino, 2014; Nishino & Willden, 2012, 2013; Ouro & Nishino, 2021; Vennell, 2012), as reviewed in Adcock et al. (2021). This theoretical approach does not consider the turbine wake; a representation as a porous disc may be used experimentally (e.g. Hachmann et al., 2021; Myers & Bahaj, 2012) or in a computational flow model in three dimensions (e.g. Roc et al., 2014).

Table 1 Levels of turbine and tidal flow models

Turbine model	Tidal model
Actuator disc models	2D depth-averaged modelling
Velocity deficit wake models	3D hydrostatic pressure model
Blade element momentum theory (BEMT) model	3D with density variation (Boussinesq)
Actuator line model (RANS or LES)	3D dynamic pressure model (RANS or LES)
Blade resolved model (RANS or LES)	With platform interaction as well as rotor
With support platform modelling, fixed and floating	With superimposed wave action

It is well known that the resulting wake velocity deficit profile over a transverse vertical plane behind the turbine may be represented as Gaussian in self-similar form (Fig. 1b, following classic theories of axi-symmetric and two-dimensional wakes (Tennekes & Lumley, 1972). The velocity deficit distribution (ΔU, given in Eq. 1) scales with the maximum normalized velocity deficit $C(x)$ and features a radial distribution $f(r/D)$ that is approximately Gaussian, with the wake centred at hub height above the bed (z_h):

$$\frac{\Delta U}{U_0} = C(x)\, f\left(\frac{r}{D}\right) = \left(1 - \sqrt{1 - \frac{C_T}{8\left(k_w \frac{x}{D} + \varepsilon\right)^2}}\right) \times \exp\left(-\frac{\left(\frac{z-z_h}{D}\right)^2 + \left(\frac{y}{D}\right)^2}{2\left(k_w \frac{x}{D} + \varepsilon\right)^2}\right) \quad (1)$$

where Cartesian x, y, z coordinates are relative to the bed below the rotor hub and other variables are defined in Fig. 1. This Gaussian model can be directly applied if the thrust coefficient (C_T) is known, which also determines the onset wake width ($\varepsilon \cdot D$). The wake diameter (D_W, Fig. 1b) grows linearly according to the wake expansion rate (k_w), proportional to the oncoming turbulence intensity, normally adopting values obtained from wind turbine wakes, as no study to date has quantified this for tidal turbines directly. Such an analytical model conserves momentum and mass flux, and has been widely used to represent the far wakes of wind turbines (Bastankhah & Porté-Agel, 2014). Similar models have been proposed for the two-dimensional far wakes of tidal turbines adopting experimental measurements (Ouro, Harrold, et al., 2019; Stallard et al., 2015).

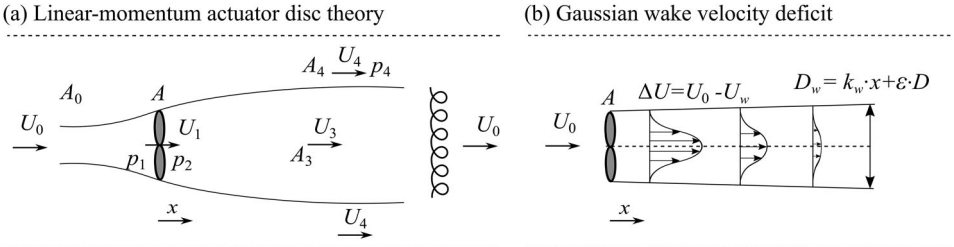

Figure 1 Theoretical representation of the wake behind a single tidal turbine adopting (a) linear-momentum actuator disc theory where U denotes streamwise velocity, A area and p pressure with a subscript denoting location (adapted from Garrett & Cummins, 2013); and (b) Gaussian wake velocity field in which ΔU denotes velocity deficit, x distance downstream of the rotor, D rotor diameter and the wake width is represented by D_w with k_w the wake expansion rate and $\varepsilon \cdot D$ the onset wake width

Linear superposition of individual velocity deficits has been shown to predict wakes of small arrays including channel blockage quite accurately (Stansby & Stallard, 2016). The local velocity at a turbine resulting from the cumulative wakes of upstream turbines determines the thrust and power for that turbine. Since power scales with the cube of velocity, the assessment of accuracy of wake superposition methods is important. Coupling such a tidal farm representation with a large scale (regional) flow model is yet to be accomplished. Whilst this paper focuses on horizontal axis turbines, the complex vertical axis turbine wakes can also be well captured by theoretical wake models using a super-Gaussian distribution that depends on the turbine's diameter and height (Ouro & Lazennec, 2021).

Actuator disc modelling may be improved by Blade Element Momentum Theory (BEMT). In this case the onset flow with axial and tangential induction factors defines the radial variation of lift and drag forces along a blade, based on quasi-steady foil coefficients, to give the average radial variation of thrust and torque on the rotor disc plane (e.g. Edmunds et al., 2017). The radial force distribution is then imposed on the computational mesh to give the flow field, accounting for possible additional effects due to blade tip losses. This permits the flow physics to be included, allowing account for swirl, and ambient and blade tip turbulence (Chapman et al., 2013; Masters et al., 2011). This approach has been applied to model turbine arrays, giving reasonable agreement between experiments and model predictions, similar to velocity deficit superposition (Olczak et al., 2016). This also allows shear in the onset flow to be accounted for.

Actuator line modelling is a more direct approach where the radial load distribution on each blade is determined in a similar way but now these individual load distributions are directly imposed on the computational mesh with forces distributed onto the neighbouring fluid cells using interpolation functions. Prandtl-like corrections at the blade tip may be also included. This approach has been successfully applied to tidal arrays (Apsley et al., 2018; Churchfield et al., 2013; Ouro & Nishino, 2021; Ouro, Ramírez, et al., 2019).

The explicit resolution of a turbine rotor requires high spatial refinement. This has been carried out using Reynolds Averaged Navier–Stokes (RANS) and large-eddy simulation (LES) approaches, with either a wall-resolved method (Afgan et al., 2013; Ahmed et al., 2017), wall-modelled method (Kang et al., 2012, 2014; McNaughton et al., 2014) or an immersed boundary method (Bai et al., 2014; Chawdhary et al., 2017; Ouro et al., 2017; Ouro & Stoesser, 2019; Posa et al., 2021; Posa & Broglia, 2021). A fine mesh related to the blades may be locally rotating at the rotor speed to avoid remeshing at every time step, as this is computationally expensive. This technique is known as a sliding mesh with boundary conditions interpolated from the fixed outer mesh to guarantee continuity between grids (Afgan et al., 2013; McNaughton et al., 2014; Tatum et al., 2016).

The approaches described above enable the support platform, stanchion, or other structural parts to be also included in the model. The detailed simulations may improve rotor design: maximizing power performance, reproducing the turbulence structures developed by the rotating turbines (Posa et al., 2021), accounting for bathymetry effects (Ouro & Stoesser, 2019), and characterizing the region of the turbine wakes (Kang et al., 2014).

Explicitly resolving the turbine rotor requires large high-performance computing (HPC) resources to run simulations within a reasonable amount of time, especially if LES is adopted as it resolves the flow scales as small as the computational mesh; this includes onset turbulence thus giving an almost fully resolved flow field (Stoesser, 2014). Simulations at this "device scale" have been limited to one or two turbines. Wall-resolved simulation requires the largest computing resources as viscous scales near the turbine blades need to be resolved. Wall-modelled boundary conditions alleviate some of the very fine resolution near the blades which also allows for larger time steps. This is similar to the immersed boundary method which has the additional advantage of decoupling the fluid and solid meshes with variables exchanged via interpolation functions.

On the other hand, actuator models allow simulation domains of up to a kilometre with a few rotors embedded providing good representation of the wake field and structural loads (Chawdhary et al., 2017, 2018; Churchfield et al., 2013; Creech et al., 2017; Ouro & Nishino, 2021).

2.2 *Tidal models*

Tidal models have been applied in civil engineering for decades, principally to simulate flooding with storm surge, sediment and contaminants transport in coastal and estuarial regions including ports, and sewage and power station outfalls, as discussed in a JHR Vision Paper on coastal hydrodynamics (Stansby, 2013). In such regions, the tidal flows may be well mixed vertically and thus depth-averaged models have been used modelling the balance between momentum, hydrostatic pressure, and bed friction with additional horizontal mixing. Such depth-averaged modelling is useful for flows with limited curvature. With prominent bathymetric features such as islands or headlands, the presence of re-circulations or wakes generally result in strong curvature, leading to unrealistic predictions of depth-averaged quantities (Stansby, 2006; Stansby et al., 2016). Three-dimensional modelling with hydrostatic pressure has also been commonplace in oceanography for decades, e.g. ROMS (Shchepetkin & McWilliams, 2005), FVCOM (Chen et al., 2003), POM (Blumberg & Mellor, 2013) and TELEMAC-3D (Hervouet, 2007). In such models, the bed boundary layer condition is modelled as well as secondary flows (due to curvature) normal to the depth-average velocity direction. Flow curvature also increases horizontal mixing and thereby bed friction due to the increased velocity gradient at the bed (Stansby, 2003). This feature determines the onset of unsteady wakes and causes less energetic eddy shedding (Stansby, 2006). The assumption of hydrostatic pressure in three dimensions for modelling complex wakes in oscillatory flow due to bathymetries of small slope has been

tested at laboratory scale with laminar flow and demonstrated to be applicable (Stansby & Lloyd, 2001). This assumption has been also shown to be effective for oscillatory headland flows with turbulence modelling, comparing with experiment (Stansby et al., 2016). For tidal flows with significant curvature due to headlands and islands, three-dimensional modelling with hydrostatic pressure is arguably a minimum requirement.

For tidal turbines, local turbulence prediction is required as it determines loading on blades, nacelle and platform, and hence fatigue life, and also drives wake recovery which determines array layout. Field measurements suggest the relative turbulence intensities of 10% to 18% depending on the site (Harrold & Ouro, 2019; Milne et al., 2016), higher than conventional values for atmospheric boundary layers. There could also be notable differences in turbulence between ebb and flood tides at the same site, depending on the velocities during each tidal phase and bathymetry (Sellar et al., 2018). These effects would be simulated with fully 3D CFD model but its use for large domains is restricted due to high computational demand.

The vertical profile of tidal velocities is normally well represented by power or logarithmic laws, although profiles of flow velocities can be more complex with highest values at mid-water depth due to bottom roughness effects or wave action (Harrold & Ouro, 2019; Lewis et al., 2021; Sellar et al., 2018). Determining both mean flow and turbulence properties are essential in building realistic inflow boundary conditions in numerical models. This is especially important if three-dimensional models are used, as robust methods that generate physics-informed artificial inflow turbulence, e.g. the synthetic eddy method (Jarrin et al., 2009; Ouro et al., 2017, 2019a), can replace the high computational cost of running precursor simulations. Input turbulence has been described in numerical models using the classical von-Karman spectrum (Parkinson & Collier, 2016) or the Kaimal spectrum proposed by the IEC standard (IEC 61400-3, 2009). In terms of turbulence anisotropy, lateral and vertical turbulence intensities (σ_v and σ_w) can be estimated from the streamwise component (σ_u) using approximate ratios $\sigma_v/\sigma_u = [0.65–0.75]$ and $\sigma_v/\sigma_u = [0.45–0.60]$. The longitudinal integral length scale can be approximated by $L_u = (zH)^{0.5}$, where z is height above the bed and H is depth (Nezu & Nakagawa, 1993), providing realistic results for tidal sites (Garcia-Novo & Kyozuka, 2019; Milne et al., 2016). The integral turbulence length scales relative to the rotor diameter at tidal sites may be expected to be smaller than those in air flows with wind turbines as rotor diameter in tidal flows may occupy a significant proportion of depth while length scales are restricted by depth in tidal flows. Detailed data on the turbulence length scales and Reynolds stresses have been reported for steady channel flow using LES in Ahmed et al. (2020), showing that the free surface only modifies the top 10% of the boundary layer formed at a solid boundary.

The bathymetry at tidal sites is often spatially heterogeneous, with the bed-generated turbulence depending on a bed roughness height and geometry. Isolated features such as rocks or deep ridges can also be found complicating the ideal deployment of tidal turbines and exacerbating the asymmetric flow distribution during ebb and flood tides (Harrold & Ouro, 2019). Shallow water models account for the bathymetry features but in most studies with 3D models a simple flat bed is adopted, as used in most laboratory experiments.

In addition, surface wave effects due to swell or wind forcing may be superimposed with tidal dynamics causing additional loading but also increased mixing.

2.3 *Wave modelling*

Traditionally the effect of currents on waves has been of prime interest when considering loading on offshore structures. This remains of concern for extreme loading on marine turbines, but we also have to account for the effect of waves on currents and turbine wakes during operational conditions. At the simplest level, wave characteristics are defined by the mean current velocity in the wave direction, with the Doppler shift determining the wave frequency in the frame of reference relative to the current giving zero mean velocity. Stokes and stream function theories up to maximum steepness may be applied for non-breaking waves (Fenton, 1985; Rienecker & Fenton, 1981). For breaking waves, the breaking forces may be considerably amplified for surface piercing bodies (Stansby et al., 2013) or floating platforms. There has been limited investigation in operational conditions but with opposing waves it has been shown through laboratory investigation that turbine thrust due to superimposed wave velocities may be simply superimposed (Fernandez-Rodriguez et al., 2014). There will also be effects on wake recovery as increased mixing may result which will improve power generation in arrays. However, there has been little study on this matter to date.

2.4 *Hydrokinetic turbines in rivers*

Tidal stream turbines, also known as hydrokinetic turbines, can be deployed in rivers with most of the same computational modelling techniques applicable to such environments. Flow in rivers is highly dependent on their morphology with the advantage of being predominantly unidirectional except at the river mouth where tides can influence the flow dynamics and become partially bi-directional (Sánchez et al., 2014). Ambient mean velocities and turbulence properties benefit from determination on-site. Deploying turbines in such environments can lead to sediment transport changes that need to be understood. Musa et al. (2018) proposed an analytical formulation to predict local scour in erodible bed surfaces around hydrokinetic devices. Chawdhary et al. (2018) performed high-resolution LES of an array of hydrokinetic turbines in the Roosevelt Island Tidal Energy Project in New York City (USA), finding that deploying 30 turbines did not make a significant disruption to the river flow. VanZwieten et al. (2015) estimated that about 120 TWh per year can be harnessed from rivers in the USA using hydrokinetic turbines. However, the shallow flow conditions determine

the turbine size and thus devices with rated capacity of only up to a few kW can be deployed. Potential applications are to supply uninterrupted renewable energy to remote and isolated communities. The rectangular cross-section of vertical axis turbines can be larger than the swept area of horizontal axis turbines, giving potential for increasing power generation.

3 Platform modelling: fixed and floating

3.1 *Fixed platforms*

Many tidal turbine developers are opting for bottom-fixed devices to minimize the influence of waves and make use of simple gravity foundations. However, at the lower part of the water column turbulence intensity is larger due to the bed influence (Mercier et al., 2020; Ouro & Stoesser, 2019) although there are lower velocities than near the free-surface. Complicated maintenance and installation operations increase operational costs. Representation of the support structure, e.g. nacelle or vertical stanchions, can be modelled as simple blockage on the mesh (Apsley et al., 2018), represented by a momentum loss (Porté-Agel et al., 2011), by adopting the immersed boundary method (Ouro et al., 2017), or by fully resolving the geometry (Mason-Jones et al., 2013; Posa & Broglia, 2021). The inclusion of the hub or nacelle determines the flow field when using actuator line models whilst the other structural components seem to have less influence on the wake (Apsley et al., 2018; Shives & Crawford, 2016). Examples of bottom-fixed turbines are those from SIMEC Atlantis, such as the AR1500 or AR2000 (https://simecatlantis.com/), NOVA Innovation (https://www.novainnovation.com/), and the decommissioned Sea-Gen that had two 600 kW rotors.

3.2 *Floating platforms*

Floating platforms for tidal turbines have several attractions. They are relatively straightforward to deploy and maintain without the need to fix to the sea bed and thus access to more sites becomes possible. Near-surface flow velocities are generally greater than near-bed velocities and thus power-generating potential is greater (as power is proportional to flow velocity cubed). There is relatively low turbulence intensity in the near-surface region too. Flow direction generally shows little variation, so the mooring alignment need not change. Floating platforms would also be preferable for large depths occurring in locations of strong ocean currents, e.g. around Taiwan and Japan, as well as tidal currents on continental shelves. The disadvantage of floating platforms is that they do require moorings subject to wave action, which may be extreme and will induce oscillating blade loads, reducing fatigue life (Mullings & Stallard, 2021).

The development of floating platforms for wind turbines is much more advanced (Carbon Trust, 2015), with semi-submersible or barge types probably closest to those for marine turbines. Time-domain methods have been developed based on BEMT for the turbine and Cummins method for linear wave diffraction-radiation theory for the platform with additional drag forces; the open-source FAST code is available from NREL (Jonkman & Buhl, 2005). There are additional second-order hydrodynamic forces due to sum and difference frequencies in the spectrum, with difference frequencies generating mean forces, and due to radiation and drag damping. The quasi-steady prediction of thrust based on relative velocity in the C_T velocity dependence has been shown to be quite close to actuator line modelling for oscillatory turbine motion (Apsley & Stansby, 2020). The linear/second-order hydrodynamic modelling may be expected to give good prediction for small to moderate waves, although oscillatory motion is still quite well predicted in large waves, while mean hydrodynamic forces may be underestimated (Stansby et al., 2019). However, the mean wind turbine thrust is significantly greater so this limitation may not be problematic. Snap mooring forces may also be underestimated. Full CFD has been undertaken by Liu et al. (2017) using OpenFOAM. The differences for marine platforms are: (1) that current is now substantial; and (2) the flow acting on the turbine may be affected by the platform while the wind turbine is mainly affected by the onset wind flow and the nacelle motion. Accounting for the effect of currents on waves due to Doppler frequency shift is important in all cases.

The question of the platform effect on rotors has been partially addressed with physical modelling using a porous disc to represent the turbine (Brown et al., 2021). For the particular Modular Tidal Generation design investigated, they found that in currents alone the turbine thrust is increased slightly by the platform ($\sim$10%). With moderate waves and currents, the mean mooring force is mainly determined by the current (unaffected by waves) and the pitch response by waves (unaffected by currents) but the cyclic loading and power from the turbine is a more complex interaction. The effect of extreme waves was not considered though. The actuator disc approach in unsteady flow due to waves with platform motion was found to give good predictions, termed weighted body force implementation (Brown, Ransley, et al., 2020). This was incorporated in OpenFOAM in a coupled model for an idealized platform of truncated cylindrical shape (Brown, Ransley, Zheng, et al., 2020).

In large waves the turbine will be parked (DNVGL, 2015) and the modelling problem is similar to that for floating wind platforms with the blades represented by a thrust on the nacelle or by actuator lines along the blades giving finer resolution. With linear diffraction-radiation-drag modelling the velocity field may be assumed to be that due to the undisturbed wave/current field as an approximation to give these forces, due to relative velocity from drag/lift coefficients. The wave field may include breaking waves and be modelled by CFD (OpenFOAM) or SPH (DualSPHysics: Domínguez et al., 2021). Nonlinear Froude–Krylov forces (due to the undisturbed pressure field) may replace linear values to give more realistic excitation forcing, which has proved effective for a single float on an

elastic mooring (Lind et al., 2016). Such approaches need to be validated against physical experiment or CFD/SPH or preferably both. In operational conditions with small wave heights the rotor represented as a porous disc may in principle be included in potential flow analysis to give hydrodynamic coefficients (e.g. WAMIT, Lee & Newman, 2013) with added viscous/drag effects. The fully coupled system may be applied as for large waves with various levels of turbine representation determining computational requirements. The motion of the platforms will affect power generation and also wake recovery which will determine array layout. With floating platforms, arrays for large-scale electricity generation have yet to be formulated.

Some of the companies developing tidal turbine in floating platforms are Orbital Marine Power with the O2 device (www.orbitalmarine.com), Sustainable Marine Energy that develops the PLAT-I power system (www.sustainablemarine.com), Modular Tidal Generators Ltd, or Magallanes Renovables with the ATIR device.

4 Present and future modelling of turbine arrays

In this section we are concerned with turbine arrays, including wake interactions, which may be considered in isolation or embedded in regional coastal models. It is desirable to model turbine wake generation with as much resolution as possible, extending as far as possible into the wake regions and for as long as possible to cover tidal cycles. Large scale modelling is challenging as turbine models represent a wide range of scales and coastal models simplify their characteristics. Here we discuss the use of such models to simulate marine turbine arrays.

4.1 *Hierarchy of models, expectations and computer resources needed*

The temporal and spatial scales of interest range from seconds ($\sim$ turbine rotation period) to hours ($\sim$ tidal phase) to days ($\sim$ monthly cycles) and from centimetres ($\sim$ turbine blade tip chord) to kilometres ($\sim$ array wakes), respectively. Figure 2 shows these temporal and spatial scales and associated modelling approaches with relevant computational times. In practice, blade-resolved RANS or LES modelling may be applied to one or two turbines only if HPC resources are available and the highest resolved array modelling has used actuator lines with modest parallel processing (8–64 cores) while coarser BEMT and actuator disc representations have been widely applied on serial processing.

Turbines have been represented in large-scale depth-integrated tidal models with parameterizations for turbine drag, thrust and support structure drag, similar to wind turbines. This approach was applied, e.g. in the finite difference model DIVAST, to investigate environmental impact of a turbine array in the Severn estuary (Ahmadian & Falconer, 2012). To account for losses due to wake mixing and blockage in cross stream turbine rows an elevation change can be imposed based on actuator disc modelling with conservation of mass and momentum (Adcock et al., 2013). This technique was incorporated in the discontinuous Galerkin model ADCIRC and applied to the Pentland Firth to give estimates of electricity generation, of about 1.9 GW. Importantly, the distinction was made between the "available" power which may be converted into electricity and the total power "extracted" from the tidal system including wake losses. Actuator disc theory can be also used to estimate equivalent bottom drag, giving power predictions (Kramer & Piggott, 2016). The 3D model with hydrostatic pressure, FVCOM, essentially an ocean model, has been applied to the Pentland Firth, assuming turbine resistance only due to turbine thrust. With this model, O'Hara Murray and Gallego (2017) found an upper limit on power generation of 5.3 GW while De Dominicis et al. (2017) found a more representative value of 1.64 GW. Similar work using Delft3D assessed the suitability of deploying tidal turbines in narrow channels characterized by complex bathymetry features (Ramos et al., 2014; Sánchez

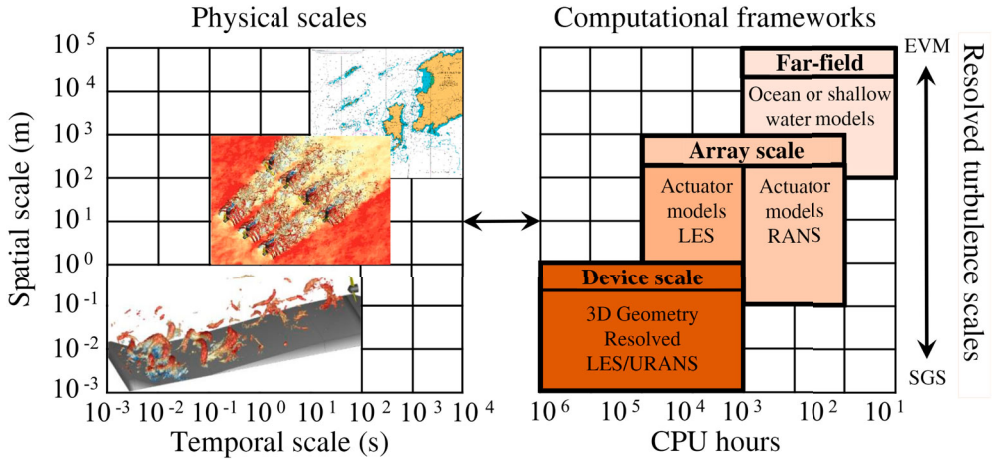

Figure 2 Interlink between physical scales of interest and available computational frameworks. The scales of resolved turbulence can range from those obtained with an eddy-viscosity model (EVM) in ocean or shallow water models to the sub-grid scales (SGS) in LES. Visualization of turbulent flow structures on the left subfigure follows from Ouro, Ramírez, et al. (2019) and Ouro, Harrold, et al. (2019).

et al., 2014). The 3D hydrostatic ROMS model with nested meshes (Shchepetkin & McWilliams, 2005) to resolve turbine wakes, with a mesh size about 10% of a turbine diameter, was applied to study turbine arrays in Fromveur Strait (western Brittany, France; Guillou et al., 2020). To reduce uncertainty in resources characterization, Lewis et al. (2021) proposed standardized curves for the power and thrust coefficients for tidal turbines based on 14 horizontal-axis designs.

The turbine representations outlined above reflect a pragmatic approach to extending functionalities already available in existing coastal/ocean models. The "elevation change actuator disc row model" for depth-averaged modelling is physically appealing but has the limitation of low flow curvature and thus is appropriate only for a small number of turbine rows. Within this constraint, such modelling systems are highly efficient. In general, the 3D hydrostatic modelling is quite accurate when used without turbines which introduce difficulties in reproducing wake mixing, important for determining effective resistance. These difficulties relate to a relatively coarse mesh, turbulence modelling appropriate for tidal flows rather than for wake conditions, and restricted vertical motion due to hydrostatic pressure assumption. It would be attractive to couple an external 3D hydrostatic model with an internal RANS or LES turbine, or array, actuator disc, BEMT or actuator line model, covering wake motion, but this has yet to be achieved.

4.2 *Towards LES as a tool for turbine array design*

At the array scale, the modeller needs to decide on the rotor representation with an actuator disc or line model and which turbulence closure to use, within RANS, LES or a hybrid of these. Most studies looking into tidal arrays, independently of the number of turbines, use RANS given it can run on laptops or workstations, whilst LES is restricted to the availability of HPC resources (Sotiropoulos, 2015), as in most applications in hydraulics or environmental flows (Stoesser, 2014). RANS closures do not resolve turbulence directly but instead model its characteristics based on the mean or slowly varying flow field. The adopted turbulence model plays a vital role in capturing the wake characteristics, e.g. shear production due to tip vortices can be underestimated with some RANS turbulence models such as standard k-ε or k-ω, thus requiring additional corrections such as SST (shear stress transport) (Apsley et al., 2018; Abolghasemi et al., 2017; Olczak et al., 2016; Shives & Crawford, 2016). LES requires high spatial resolution near the turbine, being less sensitive to the sub-grid-scale model as it resolves the turbulence length scales larger than the grid size which govern the downstream wake (Ouro & Nishino, 2021; Ouro, Ramírez, et al., 2019; Posa et al., 2021). Rotor representation in turbine arrays is normally achieved with actuator lines or disc. Typical grid resolutions that provide good estimates of performance and wake velocity field require over 40–50 grid points per rotor diameter. Lower resolution would still capture most of the wake dynamics but estimates of hydrodynamic forces can be inaccurate (Martinez-Tossas et al., 2015).

The ability of an actuator line model (ALM) to represent the flow dynamics in tidal arrays depends on the turbulence closure adopted. As an example, Fig. 3 shows the instantaneous velocity field and a vorticity iso-surface obtained adopting RANS (with the STREAM code, Apsley et al., 2018) and LES (with DOFAS code, Ouro, Harrold, et al., 2019; Ouro, Ramírez, et al., 2019) for a tidal array with three rows of three, four and five turbines per row, hub-to-hub row spacing of 1.5 diameters and four diameters between rows (Olczak et al., 2016). Note the more refined flow structures with LES. In both cases the ALM captures the tip vortices and low-velocity wake, but the former are dissipated faster in the RANS results than in those of LES. RANS then underpredicts turbulent mixing, overestimating the velocity deficit in the wake. The computing expense of LES was approximately 11,000 CPU hours running on 51 cores on a HPC facility, whilst RANS reduced the simulation time to 36 h using a 16-core workstation, equivalent to approximately 600 CPU hours. Thus, the cost of running this simulation until flow statistics are converged with LES (including Reynolds stresses) is about 20 times that taken in RANS (on same number of processors) to reach steady state values.

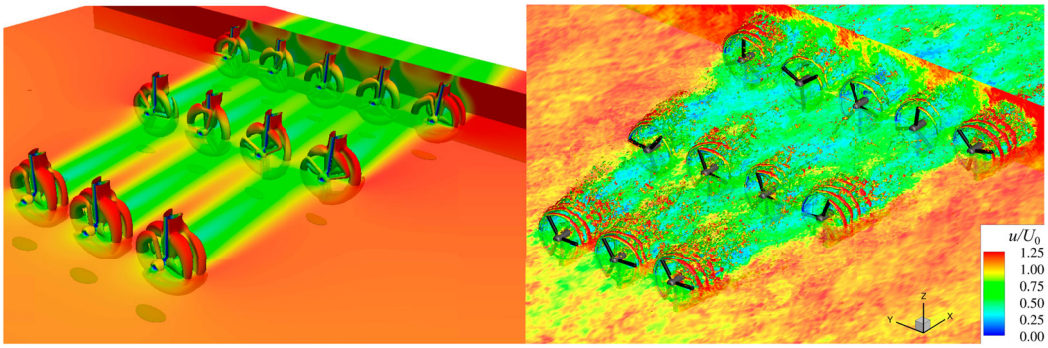

Figure 3 Simulation of a tidal stream turbine array with 12 turbines distributed in three rows. Comparison of the instantaneous streamwise velocity magnitude at hub height and on a vorticity iso-surface computed with RANS (left) using STREAM (Apsley et al., 2018) and from LES (right) using DOFAS (Ouro, Harrold, et al., 2019; Ouro, Ramírez, et al., 2019)

LES, however, remains a most valuable computational approach to resolve turbulent flows given the increasing availability of HPC resources and significant benefits in terms of the output diverse information about flow properties. The initial work on LES of tidal turbines has been mostly dedicated to single turbines to unveil the flow mechanics and obtain estimates of hydrodynamic performance. Examples of the cost of performing LES remain limited as in many publications the number of CPUs adopted or equivalent CPU hours are not reported. Nevertheless, some indications can serve as a guidance, as outlined below. Afgan et al. (2013) used 2048 cores to perform wall-resolved LES and RANS simulations using Code_SATURNE for a laboratory-scale turbine, requiring an equivalent of 4.4 and 0.14 million CPU hours respectively. Bai et al. (2014) simulated the same turbine using an immersed boundary method that allowed the reduction of the number of processors to 150. Kang et al. (2012) used 800 processors to simulate a 5 m diameter turbine. Ahmed et al. (2017) performed the LES of a 1MW devices using 4096 cores. Creech et al. (2017) performed a LES with ALM using the code Fluidity to examine the wake evolution behind the 1.2 MW two-rotor SeaGen turbine, and required more than 0.5 million CPU hours with 2400 cores. Ouro and Stoesser (2019) simulated tidal turbines operating over irregular bathymetry using 456 CPUs with an equivalent 760,000 CPU hours to provide accurate statistics of the low-frequency interaction between bed- and turbine-induced turbulence. The LES of a seven-turbine array by Ouro, Ramírez, et al. (2019) required over 50 k CPU hours using 51 cores. Posa and Broglia (2021) adopted 2048 CPUs with a major cost of 12 million core hours to capture with very high resolution the turbulent structures of the wake behind a single turbine. Ouro and Nishino (2021) computed, for the first time, LES of "infinitely long" tidal arrays using periodic boundary conditions with up to 48 turbines using 864 cores to compute approximately 1.5 h of physical time in an equivalent of 60 k CPU hours.

Most of these studies considered from one up to 48 devices modelled in relatively small spatial domains. There will be an increased computational demand when modelling planned extensive turbine arrays with over 100 devices in wider spatial domains, e.g. spanning a whole tidal channel. Thus, LES (and RANS) codes need to upscale well when increasing from hundreds to thousands of CPUs so they can efficiently model spatial domains of the order of kilometres; e.g. the consented area at MeyGen (UK) or Raz-Blanchard (France). In this context, we envisage two important considerations that will enable LES to be applied to high Reynolds number flows. First, the adoption of wall-functions to impose stresses near the tidal channel bed according to smooth or rough logarithmic velocity distributions will reduce near-wall resolution, decreasing the required number of grid cells and time step restrictions to satisfy numerical stability (based on the Courant–Friedrichs–Lewy condition). Secondly, reduced-order (actuator) models for turbine rotor representation allow the use of relatively coarse mesh grids whilst capturing the most relevant flow phenomena. Geometry-resolved approaches are unfeasible for such applications at this stage.

The accuracy of the predictions with LES relies on the adopted turbulent inflow boundary conditions, including turbulence length scale, turbulence intensity and vertical distribution of mean velocities. These can be hard to measure in the field with acoustic Doppler current profilers (ADCPs) due to the required high spatial and temporal resolution and logistical constraints. Proper uncertainty quantification can be of significant value in the prescription of turbulence at the inflow boundary conditions to provide more robust estimates of turbine array energy yield.

Despite the computational cost of LES, it provides invaluable information about the flow mechanics that can lead to developing low-order wake models based on the conventional Gaussian formulation (Bastankhah & Porté-Agel, 2014; Ouro & Lazennec, 2021; Stansby & Stallard, 2016) or by adopting data-driven approaches such as proper-orthogonal decomposition (POD) or dynamic mode decomposition (DMD) (Schmid, 2010). The latter have been used for wind turbines quite extensively to identify the most energetic flow structures present within and over the wind farm (VerHulst & Meneveau, 2014; Zhang & Stevens, 2020) but have not yet been adopted for tidal turbines. They can be used to quantify and predict phenomena such as wake meandering or changes to the wake dynamics in the presence of waves.

A relevant question to be answered in the coming years is whether LES can become a commercial tool for array design, to be added in parallel with BEMT and analytical wake models. Despite its computational cost, LES is highly beneficial as it could provide accurate estimates of wake–turbine interactions, effects of bathymetry, background turbulence, and underpin coupled models of turbine–flow interactions. Given the mostly bi-directional nature of the flow at tidal sites, few flow conditions are required to be analysed, which reduces the number of LES runs.

An example presented in Fig. 4 relates to the application of DOFAS (Ouro, Ramírez, et al., 2019) as an LES-ALM tool for the micro-siting assessment of a six-turbine array to be deployed in Bluemull Sound, Scotland (UK) by NOVA Innovation Ltd, under the EU-funded enFAIT project aimed at quantifying wake effects in a two-row array (enFAIT, 2019). The bathymetry at the site, shown in Fig. 4 (left), obtained from the free-access Emodnet database (www.emodnet-bathymetry.eu), is characterized by a large depth variation at the tidal channel centre and represented in DOFAS with an immersed boundary method. The computational domain extended 600 m by 300 m in the horizontal plane (dashed line in Fig. 4 (left)) with a uniform grid resolution of 0.25 m (yielding 36 points across the turbine rotor's diameter). The total number of grid cells is over 540 million, demanding a computational cost of about 32,000 CPU hours with 225 CPUs to simulate nearly 30 min of physical time. Due to the unavailability of turbulence characteristics at the site, only the mean flow from ADCP measurements (Macleod et al., 2019)

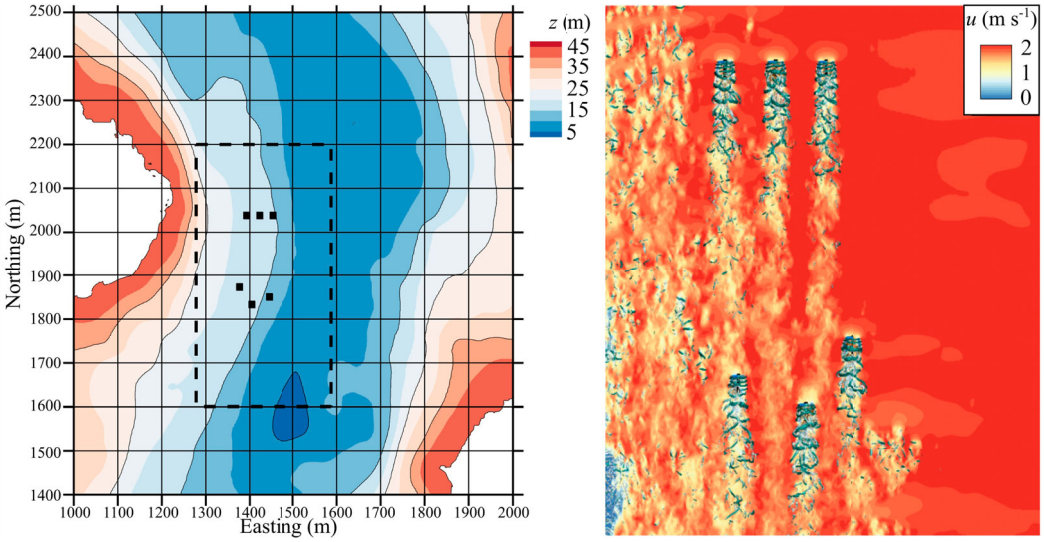

Figure 4 Left: bathymetry at Bluemull Sound (Scotland) depicting the location of the six tidal turbines and the computational domain modelled outlined with a dashed line. Right: LES results obtained with DOFAS (Ouro, Ramírez, et al., 2019) with values of instantaneous velocity and iso-surface of the vortex identification Q-criterion (Hunt et al., 1988)

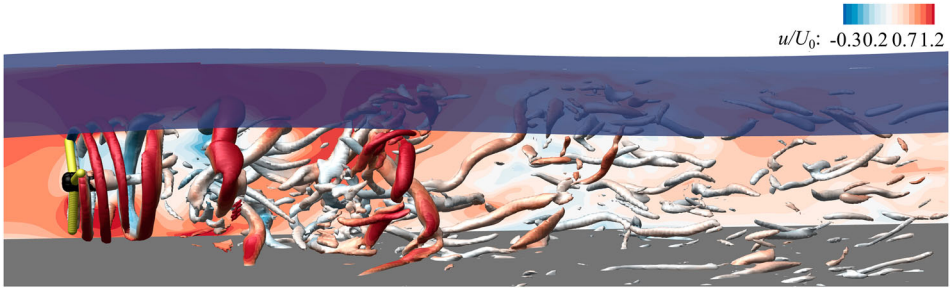

Figure 5 Instantaneous wake dynamics represented with Q-criterion iso-surfaces and contours of streamwise velocities, obtained from a LES using DOFAS (Ouro, Ramírez, et al., 2019)

with an estimated bulk velocity of approximately 2 m s^{-1} is prescribed at the inflow. Absence of turbulence at the inflow can be viewed as a worst-case scenario in which wake recovery is slowest and thus wake deficit effects remain for longer distances (Ouro et al., 2017). Rotor speed was estimated to yield a tip-speed ratio of 4.0 as a common operation point that corresponds to maximum performance. Instantaneous streamwise velocities obtained for the flood tide (north to south direction) are shown in Fig. 4 (right) capturing the interaction between the two rows of turbines spaced approximately 12 diameters apart. Bathymetry-induced turbulence is visible on the shallower region and tip vortices are also well captured.

Whilst the computational cost of using LES is high, the outputs are clearly valuable, and its explicit turbulence resolving nature provides more certainty in the results than with the turbulence modelling adopted in RANS. The key outcomes provided by DOFAS LES code include: mean wakes being aligned with the flow direction and not curved as observed from shallow water models (Macleod et al., 2019); slope of the bathymetry being large enough to cause important differences in wake recovery during ebb and flood tide with a three-turbine row simulated; a streamwise spacing between rows of 12 diameters being enough to avoid wake effects due to bathymetry-induced turbulence. The latter agrees with Ouro and Stoesser (2019) who compared LES results for a single turbine operating over a flat-bed (typical laboratory conditions) and a bathymetry with a train of dunes. Thus, LES can provide reliable estimates of improved energy yield when changing the turbines' location or hub height.

LES is also able to investigate effects of waves which may be oblique or collinear and multi-directional, as an alternative to, or reducing the scope of physical experiments. Waves may significantly affect extreme loads, fatigue and wake recovery. These effects apply to both bed mounted turbines which are sensitive to the level of submergence and floating platforms which may respond dynamically. These aspects are largely unexplored. Figure 5 shows the wake developed behind a tidal turbine modelled with ALM in presence of waves obtained with DOFAS, indicating that patches of high- and low-velocity leads to an intermittency in the wake dynamics, also affecting the coherence of tip vortices. The computational cost of explicitly resolving the air–water interface, e.g. using the level-set method (Ouro, Lopez-Novoa, et al., 2021) or volume of fluids (Tatum et al., 2016), can be deemed as approximately double that with shear-free rigid-lid conditions. The effect of array wakes on wave propagation has also yet to be assessed.

4.3 *Optimization of turbine array layout and operation*

The layout optimization is required during the design steps of large tidal turbine arrays as these will comprise (at least) dozens of devices arranged in multiple rows. Turbines in downstream rows operate in lower momentum, highly turbulent wakes generated by upstream turbines which decrease their energy yield and increase fatigue loads, depending on row spacing. The layout optimization aims at minimizing wake–turbine interaction by changing the positions of the turbines and thus maximizing the energy yield. Varying the streamwise and lateral spacing between turbines has been shown to influence the energy generation (Ouro & Nishino, 2021; Thiébot et al., 2020). Further constraints can be the limits of the spatial deployment region (i.e. consent area). Multi-objective optimization including minimization of cabling costs with cabling-routing algorithms can also be incorporated such that cost–benefit of the array is maximized (Culley et al., 2016).

Optimization algorithms require the iteration and evaluation of intermediate solutions until the optimum is found. Despite only two flow conditions being considered, i.e. ebb and flood tides, the inherent computational expense of the optimization runs restricts its use with three-dimensional models regardless of the method used to represent the turbine rotors.

Two main strategies for tidal array layout optimization prevail:

(1) Physics-informed analytical wake models, built using experimental wake measurements (Stallard et al., 2015) or high-fidelity simulations allow layout optimization with minimum computational cost, even on a standard laptop (Stansby & Stallard, 2016). This analytical wake model optimization treats each turbine and its wake individually and can be further expanded to include different operation points in order to minimize the thrust exerted by turbines, enabling downstream devices to increase their energy generation capabilities (Hachmann et al., 2021).
(2) Owing to the low computational cost of shallow water models, a continuum representation of turbine density can be adopted to optimize the array layout (Funke et al., 2014, 2015). This approach allows the optimization of the micro-siting design of tidal arrays, incorporating the impacts on the bulk channel tidal flow. This technique has been applied when considering tidal energy strategy for the Pentland Firth.

Whilst both methods provide good quantitative results for an initial assessment of an optimized layout, we envisage the need for an approach combining the physically realistic turbine wake representation with the specific features of the tidal flow at the potential deployment location, which in turn will be modified by the turbines' presence (Garcia-Novo & Kyozuka, 2021). Finally, towards a more holistic optimization approach, further refinement of the optimization procedures should incorporate design constrains such as shipping routes, deployment and maintenance costs, and ecological impacts (Vazquez & Iglesias, 2016).

Turbine control will be employed once arrays are deployed. This will be different from wind turbines as the environmental flow physics involved are different, including the presence of wave impacts. However, yaw variation of tidal turbines will be less relevant due to the predictability of the flow direction during flood and ebb tides.

4.4 *Limitations of present capability and knowledge/capability gaps*

Field and experimental data on flow–turbine interactions are scarce. Most laboratory tests have been conducted for single turbines and only few works have studied two or three devices (Stallard et al., 2013); while studies of a dozen or more turbines or porous discs are even rarer (Hachmann et al., 2021; Olczak et al., 2016). This is in contrast to wind turbine tests in which arrays with over 100 turbines have been examined in wind tunnels (Bossuyt et al., 2018).

Field data with operating tidal turbines are extremely limited. Exceptions are the field measurement campaign of the Reliable Data Acquisition Platform for Tidal (ReDAPT) project with a 1 MW turbine deployed at the tidal test site within the European Marine Energy Centre (EMEC) (Parkinson & Collier, 2016; Sellar et al., 2018), and from the DeltaStream turbine at Ramsey Sound (UK) (Harrold et al., 2020; Harrold & Ouro, 2019). Measuring wakes in the marine environment is a complex and difficult undertaking. It is still unknown how rapidly a tidal turbine wake recovers in the field, whether it is similar to the values found in the laboratory, and how the wake expansion and recovery rate varies. Such information is invaluable to quantify whether current models, such as the theoretical Gaussian model, under- or over-estimate wake effects and thus energy yield.

An additional issue to mention relates to confidentiality in rotor design by manufacturers that impose difficulties in developing research methods to account for specific details of rotors (Parkinson & Collier, 2016; Diaz-Dorado et al., 2021). It would be extremely beneficial for the tidal research to adopt a test (or benchmark) tidal turbine rotor design, as the wind turbine community has done with the NREL 5MW (Jonkman & Buhl, 2005) and now 15 MW wind turbine (Allen et al., 2020), enabling full characterization (loadings, wake evolution with current, waves, bathymetry, etc.) and encouraging cross-comparison between codes, including blind tests.

5 Current and forthcoming challenges

5.1 *Very large turbines in extensive arrays. How big may arrays be?*

Tidal arrays are expected to grow over forthcoming years both in terms of turbine number and rotor diameter. With such arrays,

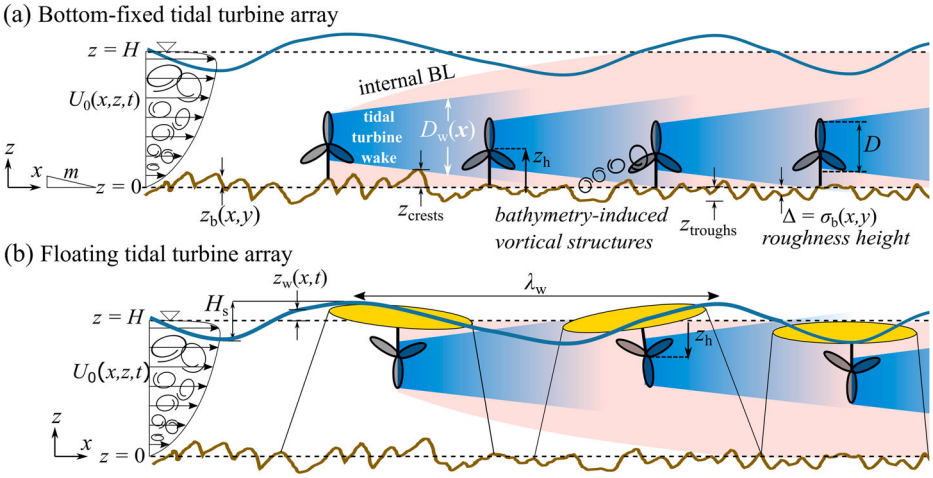

Figure 6 Schematic of the flow developed in tidal turbine arrays that are (a) bottom-fixed and (b) floating

challenges can arise from wake–turbine interactions in secondary rows that delay the recovery of mean kinetic energy across the array. Namely, an internal boundary layer is expected to be created (Fig. 6a), after the first row of turbines, that compromises the vertical fluxes of kinetic energy, key in wind farm aerodynamics (Stevens & Meneveau, 2017). Future research should look into characterizing such internal boundary layers and their role on array performance, to answer key questions: how is the kinetic energy transported through the tidal channel to be harnessed by secondary row turbines? Does this process depend on the relative submergence? Can flow energy ever be so depleted that downstream turbines have no useful resource? And, at what conditions do the tidal channel and turbine array dynamics become interdependent?

Figure 6 depicts these array-induced effects for bottom-fixed (a) and floating (b) tidal turbine arrays, in the presence of waves, irregular bathymetry (characterized by roughness height Δ and bed slope m), and individual turbine wakes. Behaviour of floating turbines in arrays with large number of devices can impact the wave field, dampening waves' effect to some degree on secondary rows.

Determining the layout of the arrays can become more important in tidal arrays compared to wind farms, with aligned and staggered arrays performing notably differently for similar turbine spacing (Ouro & Nishino, 2021).

5.2 *Wake expansion in vertically constrained environments*

Deployment sites currently under consideration for deploying tidal arrays have shallow water conditions enabling a reduction in OPEX (operating expenditure) due to faster and easier maintenance and logistics. Small ratios of water depth (H) to turbine diameter (D), if lower than 2, can lead to a delayed wake recovery behind a single turbine (Ouro, Stansby, et al., 2021), likely contributing to a reduction in power generation in back row turbines due to wake effects (Olczak et al., 2016). Thus, characterizing the wake expansion in shallow waters becomes essential to determine which sites are more suitable for arrays with a large number of turbines; e.g. MeyGen phase II has an expected 398 MW of installed capacity with approximately 100 turbines to be deployed. The magnitude of this effect is expected to be different for bottom-fixed and floating devices.

5.3 *Quantification of the impact of bathymetry*

Bathymetry effects originate from multi-scale bed roughness and non-zero slope. Irregular bathymetry is a source of turbulence that can positively contribute to a faster recovery of turbine wakes but increase the extreme loads and reduce fatigue life (Mercier et al., 2020; Ouro & Stoesser, 2019). Estimates of how wall-turbulence at a given bed roughness height (Δ in Fig. 6) drives wake recovery (e.g. wake expansion rate in theoretical models) and rotor loading would allow a better characterization of tidal sites regarding their suitability for array deployment. Effect of relative size of bedform heights in relation to the turbine diameter is another aspect to be clarified. The bed slope is also likely to impact the wake recovery of tidal turbines, as positive slope (reduction of the water depth) introduces positive pressure gradients that can accelerate momentum recovery (Shamsoddin & Porté-Agel, 2018), while a recovery delay can be experienced with negative bed slopes, i.e. with increasing water depth. Determining the threshold of the bed slope (m in Fig. 6), which, if exceeded, leads to a significant contribution to the turbine wake dynamics, has yet to be determined (Cai et al., 2021).

5.4 *Coupling of far-field coastal models and near-field RANS/LES models*

Thus far, numerical models aim at representing a well-defined range of spatio-temporal scales (Fig. 2). Large tidal arrays deployed in confined channels can lead to far-field effects that might not be captured by an array-scale model. Linking array modelling to sediment transport or water quality modelling can

also be beneficial. Coupling multi-scale and multi-process models should help in developing a holistic modelling framework adopting a near-field 3D RANS/LES model linked to a far-field 3D hydrostatic pressure model. Physical and numerical challenges will appear at coupling interfaces. They are likely to include definition of the turbulent velocity at the inflow of the near-field domain; determining synthetic turbulence quantities when transitioning from the hydrostatic pressure model to the full 3D model; definition of a sharp or buffer region at the interface between models; and efficient usage of computational resources and their synchronization required to execute parallel multi-scale simulations with codes using different grid resolution and time step integration. An alternative option is to adopt an overall hydrostatic pressure model, embedding the tidal turbine array in a small LES domain and this within a larger one resolved with RANS (Bourgoin et al., 2020). The wind energy community has made some progress in such coupling between mesoscale (atmospheric) models with microscale LES models (Hewitt et al., 2018; Porté-Agel et al., 2020).

5.5 *Hybrid tidal and wind turbine designs*

Combination of tidal turbines with wind turbines can become an attractive technology able to harness the kinetic energy from the intermittent wind and that from the predictable tidal flow with a shared platform. This wind-tidal infrastructure can yield a notable increase in energy yield (Lande-Sudall et al., 2018, 2019). Considering bottom-fixed structures, typical wind turbine monopiles have diameters similar to those of tidal turbines, leading to large momentum losses in the tidal flow (Vennell et al., 2015), which need to be considered together with blockage effects. Floating tidal-wind systems will be subjected to the thrust and loading on underwater rotors and the wind turbine. Moorings and platform stability would need to be considered in such coupled systems.

5.6 *Exascale computing: an opportunity for harnessing computational power*

In the 2010s there was a massive increase in research related to the numerical modelling of tidal stream turbines, partly attributed to the increasingly available HPC resources (Sotiropoulos, 2015). In forthcoming years, such increase and availability of HPC resources, in the so-called pre-exascale era, will hopefully enable researchers to perform simulations with higher fidelity approaches such as LES for larger spatial domains that embed tidal turbine arrays. This can enable optimization of micro-sitting of tidal turbines in consent areas to maximize energy yield by minimizing effects from wake losses, turbulence from bathymetry or wave action.

Mesh-based numerical models based on the incompressible Navier–Stokes equations are most mature. Recent numerical frameworks have arisen as possible alternatives. Smoothed particle hydrodynamics or lattice–Boltzmann methods can run on graphics processing units (GPUs) that are considerably cheaper than running simulations on multi-CPU in high-performance computing facilities (Lind et al., 2020; Mercier et al., 2020).

5.7 *Integrating numerical modelling with ecological assessments and policy*

Reliable numerical models that capture as realistically as possible the flow around tidal turbine arrays provide an opportunity to quantify the impact of this renewable energy technology on the marine ecosystem (Copping et al., 2020; Copping & Hemery, 2020; Fraser et al., 2018). This includes spatio-temporal animal distribution and species' behaviour, such as predator–prey interactions or birds foraging (Lieber et al., 2019; Williamson et al., 2022). Minimum spacing between turbines can be assessed to allow passage of marine mammals and fish, thus informing array design. Turbulence in the turbine wakes results in acoustic contamination that can disturb the aquatic fauna (Benjamins et al., 2015). Successful development of the tidal energy industry with deployment of many tidal arrays will also see large-scale array-wake effects on the regional environment as found in the offshore wind industry. Numerical models will provide an opportunity to anticipate potential energy loss when two or more arrays operate in close proximity. These aspects can inform policy both in terms of environmental impact assessment and multi array deployment (Waldman et al., 2019).

6 Conclusions

Considering large-scale engineering developments, all available analysis tools should be exploited. This is particularly the case for renewable energy generated by marine turbines in complex flows. Experiments are clearly desirable for basic understanding and validation of computational modelling, but they can be expensive, time consuming, and requiring scale effects interpretation. Unified computational modelling from blade to basin scale is not going to be practical even with exascale computing. Almost fully resolved LES modelling at blade scale is possible for one, possibly two, turbines, giving invaluable information on turbulence and wave loading and hence fatigue and extreme conditions. For modest arrays, less than 20 turbines say, actuator line modelling is practical with RANS modelling on parallel computing (say 16 cores) and with LES using HPC. The total forces acting on turbine blades may be obtained with realistic wake simulation. Synthetic turbulence may be used for input conditions. Coupling LES with regional scale 3-D tidal models which may assume hydrostatic pressure is desirable but has yet to be explored. There is considerable scope for improved modelling of floating platforms including moorings. Simulations including turbines, waves and turbulent flow remains to be undertaken in spite of high complexity and computational demands. Despite its requirement for high-performance

computing, LES is likely to become an essential tool in tidal turbine array design. LES applications would benefit from field measurements for quality assurance and thus provide capability for future array developments worldwide. Building multi-scale models seems attractive to address limitations of different numerical frameworks, underpinning cost-effective and realistic tools. Reliable numerical models can underpin future policy and environmental impact assessment for large-scale tidal energy projects.

Acknowledgements

The authors would like to thank Vladimir Nikora and Mohamed Ghidaoui for the invitation to write this Vision Paper.

Disclosure statement

No potential conflict of interest was reported by the authors.

Funding

The authors are grateful to the funding support from the UK Engineering and Physical Sciences Research Council (EPSRC) and Horizon 2020 Framework Programme from the European Union. Some of the presented material has been supported by the Dame Kathleen Ollerenshaw Fellowship that Pablo Ouro holds at the University of Manchester, and partly supported by the Tidal Stream Industry Energiser (TIGER) project, co-financed by the European Regional Development Fund through the Interreg France (Channel) England Programme.

Notation

A = area (m^2)
C_T = thrust coefficient (–)
D = rotor diameter (m)
D_w = wake diameter (m)
H = water depth (m)
H_s = surface wave height (m)
k_w = wake expansion rate (–)
m = bed gradient (–)
p = pressure (Nm^{-2})
r = radius (m)
t = time (s)
u = instantaneous horizontal velocity (ms^{-1})
U = average horizontal velocity (ms^{-1})
U_0 = upstream velocity (ms^{-1})
x = horizontal distance in streamwise direction (m)
y = horizontal distance transverse to stream direction (m)
z = vertical distance (m)
z_b = bed elevation (m)
z_{crest} = crest bed elevation (m)
z_{trough} = trough bed elevation (m)
z_h = rotor hub height above bed or below water surface
z_w = wave elevation above mean water level
ε = constant defining onset wake diameter (at $x = 0$) relative to rotor diameter (–)
Δ = bed roughness height (m)
ΔU = velocity deficit in wake (ms^{-1})
λ_w = wavelength (m)
σ_b = standard deviation of bed roughness height (m)

ORCID

Peter K. Stansby http://orcid.org/0000-0002-3552-0810
Pablo Ouro http://orcid.org/0000-0001-6411-8241

References

Abolghasemi, M. A., Piggott, M. D., Spinneken, J., Vire, A., Cotter, C. J., & Crammond, S. (2017). Simulating tidal turbines with multi-scale mesh optimisation techniques. *Journal of Fluids and Structures*, *66*, 69–90. https://doi.org/10.1016/j.jfluidstructs.2016.07.007

Adcock, T. A. A., Draper, S., Houlsby, G. T., Borthwick, A. G. L., & Serhadloglu, S. (2013). The available power from tidal stream turbines in the Pentland Firth. *Proceedings of the Royal Society A: Mathematical, Physical and Engineering Sciences*, *469*(2157), 20130072. https://doi.org/10.1098/rspa.2013.0072

Adcock, T. A. A., Draper, S., Willden, R. H. J., & Vogel, C. R. (2021). The fluid mechanics of tidal stream energy conversion. *Annual Review of Fluid Mechanics*, *53*(1), 287–310. https://doi.org/10.1146/annurev-fluid-010719-060207

Afgan, I., McNaughton, J., Rolfo, S., Apsley, D., Stallard, T., & Stansby, P. (2013). Turbulent flow and loading on a tidal stream turbine by LES and RANS. *International Journal of Heat and Fluid Flow*, *43*, 96–108. THMT special issue. https://doi.org/10.1016/j.ijheatfluidflow.2013.03.010

Ahmadian, R., & Falconer, R. A. (2012). Assessment of array shape of tidal stream turbines on hydro-environmental impacts and power output. *Renewable Energy*, *44*, 318–327. https://doi.org/10.1016/j.renene.2012.01.106

Ahmed, U., Apsley, D. D., Afgan, I., Stallard, T., & Stansby, P. K. (2017). Fluctuating loads on a tidal turbine due to velocity shear and turbulence: Comparison of CFD with field data. *Renewable Energy*, *112*, 235–246. https://doi.org/10.1016/j.renene.2017.05.048

Ahmed, U., Apsley, D., Stallard, T., Afgan, I., & Stansby, P. (2020). Turbulent length scales and budgets of Reynolds stress-transport for open-channel flows; friction Reynolds numbers ($Re\tau$) = 150, 400 and 1020. *Journal of Hydraulic Research*, *59*(1), 36–50. Forum paper. https://doi.org/10.1080/00221686.2020.1729265

Allen, C., Viselli, A., Dagher, H., Goupee, A., Gaertner, E., Abbas, N., Hall, M., & Barter, G. (2020). *Definition of the U Maine Volturn US-S reference platform developed for the IEA wind 15-Megawatt offshore reference wind turbine*. National Renewable Energy Laboratory. NREL/TP-5000-76773.

Apsley, D. D., Stallard, T., & Stansby, P. K. (2018). Actuator-line CFD modelling of tidal-stream turbines in arrays. *Journal of Ocean Engineering and Marine Energy*, *4*(4), 259–271. https://doi.org/10.1007/s40722-018-0120-3

Apsley, D. D., & Stansby, P. K. (2020). Unsteady thrust on an oscillating wind turbine: Comparison of blade-element momentum theory with actuator-line CFD. *Journal of Fluids and Structures*, *98*, 103141. https://doi.org/10.1016/j.jfluidstructs.2020.103141

Bai, X., Avital, E. J., Munjiza, A., & Williams, J. J. R. (2014). Numerical simulation of a marine current turbine in free surface flow. *Renewable Energy*, *63*, 715–723. https://doi.org/10.1016/j.renene.2013.09.042

Bastankhah, M., & Porté-Agel, F. (2014). A new analytical model for wind-turbine wakes. *Renewable Energy*, *70*, 116–123. https://doi.org/10.1016/j.renene.2014.01.002

Benjamins, S., Dale, A., Hastie, G., Waggitt, J., Lea, M.-A., Scott, B. E., & Wilson, B. (2015). Confusion reigns? A review of marine megafauna interactions with tidal-stream environments. *Oceanography and Marine Biology*, *53*, 1–54. https://doi.org/10.1201/b18733-2

Betz, A. (1920). Das Maximum der Theoretisch Möglichen Ausnützung des Windes durch Windmotoren. *Zeitschrift für das gesamte Turbinenwesen*, *26*(307–309), 8.

Blumberg, A. F., & Mellor, G. L. (2013). A description of a three-dimensional coastal ocean circulation model. In N. S. Heaps (Ed.), *Three dimensional coastal ocean models* (pp. 1–16). American Geophysical Union.

Bossuyt, J., Meneveau, C., & Meyers, J. (2018). Effect of layout on asymptotic boundary layer regime in deep wind farms. *Physical Review Fluids*, *3*(12), 124603. https://doi.org/10.1103/PhysRevFluids.3.124603

Bourgoin, A. C. L., Guillou, S. S., Thiébot, J., & Ata, R. (2020). Turbulence characterization at a tidal energy site using Large-Eddy Simulations: Case of the Alderney Race: Alderney Race turbulence les modelling. *Philosophical Transactions of the Royal Society A: Mathematical, Physical and Engineering Sciences*, *378*(2178), 20190499. https://doi.org/10.1098/rsta.2019.0499

Brown, S. A., Ransley, E. J., & Greaves, D. M. (2020). Developing a coupled turbine thrust methodology for floating tidal stream concepts: Verification under prescribed motion. *Renewable Energy*, *147*, 529–540. https://doi.org/10.1016/j.renene.2019.08.119

Brown, S. A., Ransley, E. J., Xie, N., Monk, K., De Angelis, G. M., Nicholls-Lee, R., Guerrini, E., & Greaves, D. M. (2021). On the impact of motion-thrust coupling in floating tidal energy applications. *Applied Energy*, *282*(Part B), 116246. https://doi.org/10.1016/j.apenergy.2020.116246

Brown, S. A., Ransley, E. J., Zheng, S., Xie, N., Howey, B., & Greaves, D. M. (2020). Development of a fully non-linear, coupled numerical model for assessment of floating tidal stream concepts. *Ocean Engineering*, *218*, 108253. https://doi.org/10.1016/j.oceaneng.2020.108253

Cai, T., Cheng, S., Segalini, A., & Chamorro, L. P. (2021). Local topography-induced pressure gradient effects on the wake and power output of a model wind turbine. *Theoretical and Applied Mechanics Letters*, *11*(5), 100297. https://doi.org/10.1016/j.taml.2021.100297

Carbon Trust. (2015). *Floating offshore wind: Market and technology review*.

Chapman, J. C., Masters, I., Togneri, M., & Orme, J. A. C. (2013). The Buhl correction factor applied to high induction conditions for tidal stream turbines. *Renewable Energy*, *60*, 472–480. https://doi.org/10.1016/j.renene.2013.05.018

Chawdhary, S., Angelidis, D., Colby, J., Corren, D., Shen, L., & Sotiropoulos, F. (2018). Multiresolution Large-Eddy Simulation of an array of hydrokinetic turbines in a field-scale river: The Roosevelt Island tidal energy project in New York City. *Water Resources Research*, *54*(12), 10188–10204. https://doi.org/10.1029/2018WR023345

Chawdhary, S., Hill, C., Yang, X., Guala, M., Corren, D., Colby, J., & Sotiropoulos, F. (2017). Wake characteristics of a TriFrame of axial-flow hydrokinetic turbines. *Renewable Energy*, *109*, 332–345. https://doi.org/10.1016/j.renene.2017.03.029

Chen, C., Liu, H., & Beardsley, R. C. (2003). An unstructured grid, finite-volume, three-dimensional, primitive equations ocean model: Application to coastal ocean and estuaries. *Journal of Atmospheric and Oceanic Technology*, *20*(1), 159–186. https://doi.org/10.1175/1520-0426(2003)020<0159:AUGFVT>2.0.CO;2

Churchfield, M. J., Li, Y., & Moriarty, P. J. (2013). A Large-Eddy Simulation study of wake propagation and power production in an array of tidal-current turbines. *Philosophical Transactions of the Royal Society A: Mathematical, Physical and Engineering Sciences*, *371*(1985), 20120421. https://doi.org/10.1098/rsta.2012.0421

Coles, D., Angeloudis, A., Greaves, D., Hastie, G., Lewis, M., Mackie, L., McNaughton, J., Miles, J., Neill, S., Piggott, M., Risch, D., Scott, B., Sparling, C., Stallard, T., Thies, P., Walker, S., White, D., Willden, R., & Williamson, B. (2021). A review of the UK and British Channel Islands practical tidal stream energy resource subject areas. *Philosophical Transactions of the Royal Society A*, *477*(2255), 20210469. https://doi.org/10.1098/rspa.2021.0469

Copping, A. E., & Hemery, L. G. (2020). *OES-environmental 2020 state of the science report: Environmental effects of marine renewable energy development around the world*. Report for Ocean Energy Systems (OES).

Copping, A. E., Hemery, L. G., Overhus, D. M., Garavelli, L., Freeman, M. C., Whiting, J. M., Gorton, A. M., Farr, H. K., Rose, D. J., & Tugade, L. G. (2020). Potential environmental

effects of marine renewable energy development—the state of the science. *Journal of Marine Science and Engineering*, *8*(11), 879. https://doi.org/10.3390/jmse8110879

Creech, A. C. W., Borthwick, A. G. L., & Ingram, D. (2017). Effects of support structures in an LES actuator line model of a tidal turbine with contra-rotating rotors. *Energies*, *10*(5), 726. https://doi.org/10.3390/en10050726

Culley, D. M., Funke, S. W., Kramer, S. C., & Piggott, M. D. (2016). Integration of cost modelling within the micro-siting design optimisation of tidal turbine arrays. *Renewable Energy*, *85*, 215–227. https://doi.org/10.1016/j.renene.2015.06.013

De Dominicis, M., O'Hara Murray, R., & Wolf, J. (2017). Multi-scale ocean response to a large tidal stream turbine array. *Renewable Energy*, *114*, 1160–1179. https://doi.org/10.1016/j.renene.2017.07.058

DNVGL. (2015) Standard DNVGL-ST-0164 Tidal turbines (edition October 2015).

Domínguez, J. M., Fourtakas, G., Altomare, C., Canelas, R. B., Tafuni, A., García-Feal, O., Martínez-Estévez, I., Mokos, A., Vacondio, R., Crespo, A. J. C., Rogers, B. D., Stansby, P. K., & Gómez-Gesteira, M. (2021). DualSPHysics: From fluid dynamics to multi-physics problems. *Computational Particle Mechanics*. https://doi.org/10.1007/s40571-021-00404-2

Draper, S., & Nishino, T. (2014). Centred and staggered arrangements of tidal turbines. *Journal of Fluid Mechanics*, *739*, 72–93. https://doi.org/10.1017/jfm.2013.593

Edmunds, M., Williams, A., Masters, I., & Croft, T. N. (2017). An enhanced disk averaged CFD model for the simulation of horizontal axis tidal turbines. *Renewable Energy*, *101*, 67–81. https://doi.org/10.1016/j.renene.2016.08.007

enFAIT (Enabling Future Arrays in Tidal). (2019). enFAIT-EU-0004 test plan report.

Fenton, J. D. (1985). A fifth-order Stokes theory for steady waves. *Journal of Waterway, Port, Coastal, and Ocean Engineering*, *111*(2), 216–234. https://doi.org/10.1061/(ASCE)0733-950X(1985)111:2(216)

Fernandez-Rodriguez, E., Stallard, T. J., & Stansby, P. K. (2014). Experimental study of extreme thrust on a tidal stream rotor due to turbulent flow and with opposing waves. *Journal of Fluids and Structures*, *51*, 354–361. https://doi.org/10.1016/j.jfluidstructs.2014.09.012

Fraser, S., Williamson, B. J., Nikora, V., & Scott, B. E. (2018). Fish distributions in a tidal channel indicate the behavioural impact of a marine renewable energy installation. *Energy Reports*, *4*, 65–69. https://doi.org/10.1016/j.egyr.2018.01.008

Funke, S. W., Farrell, P. E., & Piggott, M. D. (2014). Tidal turbine array optimisation using the adjoint approach. *Renewable Energy*, *63*, 658–673. https://doi.org/10.1016/j.renene.2013.09.031

Funke, S. W., Farrell, P. E., & Piggott, M. D. (2015). Design optimisation and resource assessment for tidal-stream renewable energy farms using a new continuous turbine approach. *Renewable Energy*, *99*, 1046–1061. https://doi.org/10.1016/j.renene.2016.07.039

Garcia-Novo, P., & Kyozuka, Y. (2019). Analysis of turbulence and extreme current velocity values in a tidal channel. *Journal of Marine Science and Technology*, *24*(3), 659–672. https://doi.org/10.1007/s00773-018-0601-z

Garcia-Novo, P., & Kyozuka, Y. (2021). Tidal stream energy as a potential continuous power producer: A case study for West Japan. *Energy Conversion and Management*, *245*, 114533. https://doi.org/10.1016/j.enconman.2021.114533

Garrett, C., & Cummins, P. (2013). Maximum power from a turbine farm in shallow water. *Journal of Fluid Mechanics*, *714*, 634–643. https://doi.org/10.1017/jfm.2012.515

Glauert, H. (1935). Airplane propellers. In W. F. Durand (Ed.), *Aerodynamic theory* (Vol. *IV*, pp. 169–360). Springer.

Guillou, N., Charpentier, J.-F., & Benbouzid, M. (2020). The Tidal stream energy resource of the Fromveur Strait—a review. *Journal of Marine Science and Engineering*, *8*(12), 1037. https://doi.org/10.3390/jmse8121037

Hachmann, C., Stallard, T., Stansby, P., & Lin, B. (2021). Experimentally validated study of the impact of operating strategies on power efficiency of a turbine array in a bi-directional tidal channel. *Renewable Energy*, *163*, 1408–1426. https://doi.org/10.1016/j.renene.2020.06.090

Harrold, M., & Ouro, P. (2019). Rotor loading characteristics of a full-scale tidal turbine. *Energies*, *12*(6), 1035. https://doi.org/10.3390/en12061035

Harrold, M., Ouro, P., & O'Doherty, T. (2020). Performance assessment of a tidal turbine using two flow references. *Renewable Energy*, *153*, 624–633. https://doi.org/10.1016/j.renene.2019.12.052

Hervouet, J.-M. (2007). *Hydrodynamics of free surface flows modelling with the finite element method*. Wiley (360 pp).

Hewitt, S., Margetts, L., & Revell, A. (2018). Building a digital wind farm. *Archives of Computational Methods in Engineering*, *25*(4), 879–899. https://doi.org/10.1007/s11831-017-9222-7

Hunt, J., Wray, A., & Moin, P. (1988). *Eddies, streams, and convergence zone in turbulent flows*. *Proceedings of the summer program, report CTR-S88, NASA Stanford center for turbulence research, 1988*, pp. 193–208.

IEC 61400-3. (2009). *Wind turbines – Part 3: Design requirements for offshore wind turbines*. IEC Standard.

Jarrin, N., Prosser, N., Uribe, J. C., Benhamadouche, S., & Laurence, D. (2009). Reconstruction of turbulent fluctuations for hybrid RANS/LES simulations using a Synthetic-Eddy Method. *International Journal of Heat and Fluid Flow*, *30*(3), 435–442. https://doi.org/10.1016/j.ijheatfluidflow.2009.02.016

Jonkman, J. M., & Buhl Jr, M. L. (2005). *FAST user's guide*. Tech. Rep. NREL/EL-500-29798, National Renewable Energy Laboratory, Golden, Colorado.

Kang, S., Borazjani, I., Colby, J. A., & Sotiropoulos, F. (2012). Numerical simulation of 3D flow past a real-life marine

hydrokinetic turbine. *Advances in Water Resources*, *39*, 33–43. https://doi.org/10.1016/j.advwatres.2011.12.012

Kang, S., Yang, X., & Sotiropoulos, F. (2014). On the onset of wake meandering for an axial flow turbine in a turbulent open channel flow. *Journal of Fluid Mechanics*, *744*, 376–403. https://doi.org/10.1017/jfm.2014.82

Kramer, S. C., & Piggott, M. D. (2016). A correction to the enhanced bottom drag parameterisation of tidal turbines. *Renewable Energy*, *92*, 385–396. https://doi.org/10.1016/j.renene.2016.02.022

Lande-Sudall, D., Stallard, T., & Stansby, P. (2018). Co-located offshore wind and tidal stream turbines: Assessment of energy yield and loading. *Renewable Energy*, *118*, 627–643. https://doi.org/10.1016/j.renene.2017.10.063

Lande-Sudall, D., Stallard, T., & Stansby, P. (2019). Co-located deployment of offshore wind turbines with tidal stream turbine arrays for improved cost of electricity generation. *Renewable and Sustainable Energy Reviews*, *104*, 492–503. https://doi.org/10.1016/j.rser.2019.01.035

Lee, C. H., & Newman, J. N. (2013). *WAMIT – user manual version 7.0*. WAMIT Inc.

Lewis, M., O'Hara Murray, R., Fredriksson, S., Maskell, J., de Fockert, A., Neill, S. P., & Robins, P. E. (2021). A standardised tidal-stream power curve, optimised for the global resource. *Renewable Energy*, *170*, 1308–1323. https://doi.org/10.1016/j.renene.2021.02.032

Lieber, L., Nimmo-Smith, W. A. M., Waggitt, J. J., & Kregting, L. (2019). Localised anthropogenic wake generates a predictable foraging hotspot for top predators. *Communications Biology*, *2*(1), 12–13. https://doi.org/10.1038/s42003-019-0364-z

Lind, S. J., Rogers, B. D., & Stansby, P. K. (2020). Review of smoothed particle hydrodynamics: Towards converged Lagrangian flow modelling. *Proceedings of the Royal Society A: Mathematical, Physical and Engineering Sciences*, *476*(2241), 20190801. https://doi.org/10.1098/rspa.2019.0801

Lind, S. J., Stansby, P. K., & Rogers, B. D. (2016). Fixed and moored bodies in steep and breaking waves using SPH with the Froude Krylov approximation. *Journal of Ocean Engineering and Marine Energy*, *2*(3), 331–354. https://doi.org/10.1007/s40722-016-0056-4

Liu, Y., Xiao, Q., Incecik, A., Peyrard, C., & Wan, D. (2017). Establishing a fully coupled CFD analysis tool for floating offshore wind turbines. *Renewable Energy*, *112*, 280–301. https://doi.org/10.1016/j.renene.2017.04.052

Macleod, A., Watson, A., Quantrell, D., Porteous, S., & Wills, T. (2019). *Tidal resource, turbine wake and performance modelling on the EnFAIT project. 13th European Wave and Tidal Energy Conference (EWTEC)*, Naples, Italy.

Martinez-Tossas, L., Churchfield, M., & Leonardi, S. (2015). Large Eddy Simulations of the flow past wind turbines: Actuator line and disk modelling. *Wind Energy*, *18*(6), 1047–1060. https://doi.org/10.1002/we.1747

Mason-Jones, A., O'Doherty, D. M., Morris, C. E., & O'Doherty, T. (2013). Influence of a velocity profile & support structure on tidal stream turbine performance. *Renewable Energy*, *52*, 23–30. https://doi.org/10.1016/j.renene.2012.10.022

Masters, I., Chapman, J. C., Orme, J. A. C., & Willis, M. R. (2011). A robust blade element momentum theory model for tidal stream turbines including tip and hub loss corrections. *Proceedings of the Institution of Mechanical Engineers, Part C*, *10*, 25–35. https://doi.org/10.1080/20464177.2011.11020241

McNaughton, J., Afgan, I., Apsley, D. D., Rolfo, S., Stallard, T., & Stansby, P. K. (2014). A simple sliding-mesh interface procedure and its application to the CFD simulation of a tidal-stream turbine. *International Journal for Numerical Methods in Fluids*, *74*(4), 250–269. https://doi.org/10.1002/fld.3849

Mercier, P.,Grondeau, M., Guillou, S., Thiébot, J., & Poizot, E. (2020). Numerical study of the turbulent eddies generated by the seabed roughness. Case study at a tidal power site. *Applied Ocean Research*, *97*, 102082. https://doi.org/10.1016/j.apor.2020.102082

Milne, I. A., Day, A. H., Sharma, R. N., & Flay, R. G. J. (2016). The characterisation of the hydrodynamic loads on tidal turbines due to turbulence. *Renewable and Sustainable Energy Reviews*, *56*, 851–864. https://doi.org/10.1016/j.rser.2015.11.095

Mullings, H., & Stallard, T. (2021). Assessment of dependency of unsteady onset flow and resultant tidal turbine fatigue loads on measurement position at a tidal site. *Energies*, *14*(17), 5470. https://doi.org/10.3390/en14175470

Musa, M., Heisel, M., & Guala, M. (2018). Predictive model for local scour downstream of hydrokinetic turbines in erodible channels. *Physical Review Fluids*, *3*(2), 024606. https://doi.org/10.1103/PhysRevFluids.3.024606

Myers, L. E., & Bahaj, A. S. (2012). An experimental investigation simulating flow effects in first generation marine current energy converter arrays. *Renewable Energy*, *37*(1), 28–36. https://doi.org/10.1016/j.renene.2011.03.043

Nezu, I., & Nakagawa, H. (1993). *Turbulence in open-channel flows*. IAHR-Monograph. Balkema.

Nishino, T., & Willden, R. H. J. (2012). The efficiency of an array of tidal turbines partially blocking a wide channel. *Journal of Fluid Mechanics*, *708*, 596–606. https://doi.org/10.1017/jfm.2012.349

Nishino, T., & Willden, R. H. J. (2013). Two-scale dynamics of flow past a partial cross-stream array of tidal turbines. *Journal of Fluid Mechanics*, *730*, 220–244. https://doi.org/10.1017/jfm.2013.340

Offshore Energy. (2015). *Estimate of global potential tidal resources*. https://www.offshore-energy.biz/estimate-of-global-potential-tidal-resources/.

O'Hara Murray, R., & Gallego, A. (2017). A modelling study of the tidal stream resource of the Pentland Firth, Scotland. *Renewable Energy*, *102*, 326–340. https://doi.org/10.1016/j.renene.2016.10.053

Olczak, A., Stallard, T., Feng, T., & Stansby, P. K. (2016). Comparison of a RANS blade element model for tidal turbine arrays with laboratory scale measurements of wake velocity and rotor thrust. *Journal of Fluids and Structures*, *64*, 87–106. https://doi.org/10.1016/j.jfluidstructs.2016.04.001

Ouro, P., Harrold, M., Ramírez, L., & Stoesser, T. (2019). Prediction of the wake behind a horizontal axis tidal turbine using a LES-ALM. In Esteban Ferrer & Adeline Montlaur (Eds.), *Prog. CFD wind tidal offshore turbines* (pp. 25–35). Springer.

Ouro, P., Harrold, M., Stoesser, T., & Bromley, P. (2017). Hydrodynamic loadings on a horizontal axis tidal turbine prototype. *Journal of Fluids and Structures*, *71*, 78–95. https://doi.org/10.1016/j.jfluidstructs.2017.03.009

Ouro, P., & Lazennec, M. (2021). Theoretical modelling of the three-dimensional wake of vertical axis turbines. *Flow*, *1*, E3. https://doi.org/10.1017/flo.2021.4

Ouro, P., Lopez-Novoa, U., & Guest, M. (2021). On the performance of a highly-scalable Computational Fluid Dynamics code on AMD, ARM and Intel processor-based HPC systems. *Computer Physics Communications*, *269*, 108105. https://doi.org/10.1016/j.cpc.2021.108105

Ouro, P., & Nishino, T. (2021). Performance and wake characteristics of tidal turbines in an infinitely large array. *Journal of Fluid Mechanics*, *925*, A30. https://doi.org/10.1017/jfm.2021.692

Ouro, P., Ramírez, L., & Harrold, M. (2019). Analysis of array spacing on tidal stream turbine farm performance using Large-Eddy Simulation. *Journal of Fluids and Structures*, *91*, 102732. https://doi.org/10.1016/j.jfluidstructs.2019.102732

Ouro, P., Stansby, P., & Stallard, T. (2021). *Investigation of the wake recovery behind a tidal stream turbine for various submergence levels*. *14th European Wave and Tidal Energy Conference (EWTEC)*, Plymouth, UK.

Ouro, P., & Stoesser, T. (2019). Impact of environmental turbulence on the performance and loadings of a tidal stream turbine. *Flow, Turbulence and Combustion*, *102*(3), 613–639. https://doi.org/10.1007/s10494-018-9975-6

Parkinson, S., & Collier, W. (2016). Model validation of hydrodynamic loads and performance of a full-scale tidal turbine using Tidal Bladed. *International Journal of Marine Energy*, *16*(279), 297. https://doi.org/10.1016/j.ijome.2016.08.001

Porté-Agel, F., Bastankhah, S., & Shamsoddin, S. (2020). Wind-turbine and wind-farm flows: A review. *Boundary-Layer Meteorology*, *174*(1), 1–59. https://doi.org/10.1007/s10546-019-00473-0

Porté-Agel, F., Wu, Y. T., Lu, H., & Conzemius, R. J. (2011). Large-Eddy Simulation of atmospheric boundary layer flow through wind turbines and wind farms. *Journal of Wind Engineering and Industrial Aerodynamics*, *99*(4), 154–168. https://doi.org/10.1016/j.jweia.2011.01.011

Posa, A., & Broglia, R. (2021). Characterization of the turbulent wake of an axial-flow hydrokinetic turbine via Large-Eddy Simulation. *Computers & Fluids*, *216*, 104815. https://doi.org/10.1016/j.compfluid.2020.104815

Posa, A., Broglia, R., & Balaras, E. (2021). Instability of the tip vortices shed by an axial-flow turbine in uniform flow. *Journal of Fluid Mechanics*, *920*, A19. https://doi.org/10.1017/jfm.2021.433

Ramos, V., Carballo, R., Sánchez, M., Veigas, M., & Iglesias, G. (2014). Tidal stream energy impacts on estuarine circulation. *Energy Conversion and Management*, *80*, 137–149. https://doi.org/10.1016/j.enconman.2014.01.027

Rienecker, M. M., & Fenton, J. D. (1981). A Fourier approximation method for steady water waves. *Journal of Fluid Mechanics*, *104*, 119–137. https://doi.org/10.1017/S0022112081002851

Roc, T., Greaves, D. M., Thyng, M., & Conley, D. C. (2014). Tidal turbine representation in an ocean circulation model: Towards realistic applications. *Ocean Engineering*, *78*, 95–111. https://doi.org/10.1016/j.oceaneng.2013.11.010

Sánchez, M., Carballo, R., Ramos, V., & Iglesias, G. (2014). Tidal stream energy impact on the transient and residual flow in an estuary: A 3D analysis. *Applied Energy*, *116*, 167–177. https://doi.org/10.1016/j.apenergy.2013.11.052

Schmid, P. J. (2010). Dynamic mode decomposition of numerical and experimental data. *Journal of Fluid Mechanics*, *656*, 5–28. https://doi.org/10.1017/S0022112010001217

Sellar, B. G., Wakelam, G., Sutherland, D. R. J., Ingram, D. M., & Venugopal, V. (2018). Characterisation of tidal flows at the European Marine Energy Centre in the absence of ocean waves. *Energies*, *11*(1), 176–123. https://doi.org/10.3390/en11010176

Shamsoddin, S., & Porté-Agel, F. (2018). A model for the effect of pressure gradient on turbulent axisymmetric wakes. *Journal of Fluid Mechanics*, *837*, R3. https://doi.org/10.1017/jfm.2017.864

Shchepetkin, A. F., & McWilliams, J. C. (2005). The regional oceanic modelling system (ROMS): A split-explicit, free-surface, topography-following-coordinate oceanic model. *Ocean Modelling*, *9*(4), 347–404. https://doi.org/10.1016/j.ocemod.2004.08.002

Shives, M., & Crawford, C. (2016). Adapted two-equation turbulence closures for actuator disk RANS simulations of wind & tidal turbine wakes. *Renewable Energy*, *92*, 273–292. https://doi.org/10.1016/j.renene.2016.02.026

Sotiropoulos, F. (2015). Hydraulics in the era of exponentially growing computing power. *Journal of Hydraulic Research*, *53*(5), 547–560. https://doi.org/10.1080/00221686.2015.1119210

Stallard, T. J., Collings, R., Feng, T., & Whelan, J. (2013). Interactions between tidal turbine wakes: Experimental

study of a group of three-bladed rotors. *Philosophical Transactions of the Royal Society A: Mathematical, Physical and Engineering Sciences*, *371*(1985), 20120159. https://doi.org/10.1098/rsta.2012.0159

Stallard, T. J., Feng, T., & Stansby, P. K. (2015). Experimental study of the mean wake of a tidal stream rotor in a shallow turbulent flow. *Journal of Fluids and Structures*, *54*, 235–246. https://doi.org/10.1016/j.jfluidstructs.2014.10.017

Stansby, P., Chini, N., & Lloyd, P. (2016). Oscillatory flows around a headland by 3D modelling with hydrostatic pressure and implicit bed shear stress comparing with experiment and depth-averaged modelling. *Coastal Engineering*, *116*, 1–14. https://doi.org/10.1016/j.coastaleng.2016.05.008

Stansby, P. K. (2003). A mixing-length model for shallow turbulent wakes. *Journal of Fluid Mechanics*, *495*, 369–384. https://doi.org/10.1017/S0022112003006384

Stansby, P. K. (2006). Limitations of depth-averaged modelling of shallow wakes. *Journal of Hydraulic Engineering*, *132*(7), 737–740. https://doi.org/10.1061/(ASCE)0733-9429(2006)132:7(737)

Stansby, P. K. (2013). Coastal hydrodynamics – present and future. *Journal of Hydraulic Research*, *51*(4), 341–350. https://doi.org/10.1080/00221686.2013.821678

Stansby, P. K., Carpintero Moreno, E., Apsley, D. D., & Stallard, T. J. (2019). Slack-moored semi-submersible wind floater with damping plates in waves: Linear diffraction modelling with mean forces and experiments. *Journal of Fluids and Structures*, *90*, 410–431. https://doi.org/10.1016/j.jfluidstructs.2019.07.010

Stansby, P. K., Devaney, L. C., & Stallard, T. J. (2013). Breaking wave loads on monopiles for offshore wind turbines and estimation of extreme overturning moment. *IET Renewable Power Generation*, *7*(5), 514–520. https://doi.org/10.1049/iet-rpg.2012.0205

Stansby, P. K., & Lloyd, P. M. (2001). Wake formation around islands in oscillatory laminar shallow-water flows: Part II 3-D boundary-layer modelling. *Journal of Fluid Mechanics*, *429*, 239–254. https://doi.org/10.1017/S0022112000002834

Stansby, P., & Stallard, T. (2016). Fast optimisation of tidal stream turbine positions for power generation in small arrays with low blockage based on superposition of self-similar far-wake velocity deficit profiles. *Renewable Energy*, *92*, 366–375. https://doi.org/10.1016/j.renene.2016.02.019

Stevens, R.J.A.M., & Meneveau, C. (2017). Flow Structure and Turbulence in Wind Farms. *Annual Review of Fluid Mechanics*, *49*, 311–339. https://doi.org/10.1146/annurev-fluid-010816-060206

Stoesser, T. (2014). Large-Eddy Simulation in hydraulics: Quo Vadis? *Journal of Hydraulic Research*, *52*(4), 441–452. https://doi.org/10.1080/00221686.2014.944227

Tatum, S., Frost, C., Allmark, M., O'Doherty, D. M., Mason-Jonse, A., Prickett, P. W., Grosvenor, R. I., Bryen, C. B., & O'Doherty, T. (2016). Wave-current interaction effects on tidal stream turbine performance and loading characteristics. *International Journal of Marine Energy*, *14*, 161–179. https://doi.org/10.1016/j.ijome.2015.09.002

Tennekes, H., & Lumley, J. (1972). *A first course in turbulence*. The MIT Press.

Thiébot, J., Guillou, N., Guillou, S., Good, A., & Lewis, M. (2020). Wake field study of tidal turbines under realistic flow conditions. *Renewable Energy*, *151*, 1196–1208. https://doi.org/10.1016/j.renene.2019.11.129

VanZwieten, J., McAnally, W., Ahmad, J., Davis, T., Martin, J., Bevelhimer, M., Cribbs, A., Lippert, R., Hudon, T., & Trudeau, M. (2015). In-stream hydrokinetic power: Review and appraisal. *Journal of Energy Engineering*, *141*(3), 04014024. https://doi.org/10.1061/(ASCE)EY.1943-7897.0000197

Vazquez, A., & Iglesias, G. (2016). A holistic method for selecting tidal stream energy hotspots under technical, economic and functional constraints. *Energy Conversion and Management*, *117*, 420–430. https://doi.org/10.1016/j.enconman.2016.03.012

Vennell, R. (2012). The energetics of large tidal turbine arrays. *Renewable Energy*, *48*, 210–219. https://doi.org/10.1016/j.renene.2012.04.018

Vennell, R., Funke, S. W., Draper, S., Stevens, C., & Divett, T. (2015). Designing large arrays of tidal turbines: A synthesis and review. *Renewable and Sustainable Energy Reviews*, *41*, 454–472. https://doi.org/10.1016/j.rser.2014.08.022

VerHulst, C., & Meneveau, C. (2014). Large Eddy Simulation study of the kinetic energy entrainment by energetic turbulent flow structures in large wind farms. *Physics of Fluids*, *26*(2), 025113. https://doi.org/10.1063/1.4865755

Waldman, S., Weir, S., O'Hara Murray, R. B., Woolf, D. K., & Kerr, S. (2019). Future policy implications of tidal energy array interactions. *Marine Policy*, *108*, 103611. https://doi.org/10.1016/j.marpol.2019.103611

Williamson, L. D., Scott, B. E., Laxton, M. R., Bachl, F. E., Illian, J. B., Brookes, K. L., & Thompson, P. M. (2022). Spatio-temporal variation in harbor porpoise distribution and foraging across a landscape of fear. *Marine Mammal Science*, *38*, 42–57. https://doi.org/10.1111/mms.12839

Zhang, M., & Stevens, R. (2020). Characterizing the coherent structures within and above large wind farms. *Boundary-Layer Meteorology*, *174*(1), 61–80. https://doi.org/10.1007/s10546-019-00468-x